PHOTOSYNTHETICA 42 (3): 417-423, 2004

Effects of potato virus Y^{NTN} infection on gas exchange and photosystem 2 function in leaves of *Solanum tuberosum* L.

Y.H. ZHOU[*], Y.H. PENG[*], J.L. LEI[*], L.Y. ZOU[*], J.H. ZHENG[*], and J.Q. YU[*,**,***]

Horticultural Department, Huajiachi Campus, Zhejiang University, Hangzhou 310029, P.R. China[*]
Laboratory of Horticultural Plant Growth, Development and Biotechnology, Ministry of Agriculture, Hangzhou 310029, P.R. China[**]

Abstract

Photosynthetic responses of potato (*Solanum tuberosum* L. cv. Chunzao) were examined during potato virus Y (PVY^{NTN}) infection. PVY^{NTN} infection significantly reduced net photosynthetic rate and stomatal conductance, but had little influence on intercellular CO_2 concentration. As the disease developed, the maximum carboxylation velocity of ribulose-1,5-bisphosphate carboxylase/oxygenase and the maximum electron transport rate contributing to ribulose-1,5-bisphosphate regeneration gradually decreased, followed by substantial reductions in the relative quantum efficiency of photosystem 2 (PS2) electron transport, the efficiency of excitation energy capture by open PS2 reaction centres, and photochemical quenching, but not in sustained photoinhibition. Thus PVY^{NTN} depressed photosynthesis mainly by interfering with the enzymatic processes in the Calvin cycle which resulted in a down-regulation of electron transport.

Additional key words: chlorophyll fluorescence; intercellular CO_2 concentration; net photosynthetic rate; photochemistry; photosynthetic electron transport; potato; potato virus Y; quantum yield; stomatal conductance.

Introduction

Potato virus Y (PVY^{NTN}) is prevalent in potato plants. It infects potato leaves and spreads rapidly. PVY^{NTN} results in a great loss of yield and is a world-wide problem in the potato production (Dolenc *et al.* 2000). Virus-infected plants show strong morphological and physiological alterations, with symptoms such as leaf mosaic and curling or vein necrosis associated with changes in the chloroplast structure and function (Reinero and Beachy 1989, Rahoutei *et al.* 2000, Pompe-Novak *et al.* 2001). Previous studies show that lowered plant growth rate in virus-infected plants is attributed mainly to impaired photosynthesis in virus-infected leaves with reduced chlorophyll (Chl) content and maximum Chl fluorescence, decreased activities of some photosynthetic enzymes, and elevated sugar or starch contents (Montalbini and Lupattelli 1989, Funayama *et al.* 1997, Osmond *et al.* 1998, Funayama and Terashima 1999, Swiech *et al*. 2001). Effects of virus infection on photosynthesis have been mostly studied in the tobacco mosaic virus (TMV) systems (Montalbini and Lupattelli 1989, Balachandran and Osmond 1994, Balachandran *et al.* 1994, 1997, Wolf and Millatiner 2000). The coat protein of TMV is bound to photosystem 2 (PS2) complex with lowered activities of PS2 electron transport (Reinero and Beachy 1989) and induces chronic photoinhibition, which leads to yellow mosaic symptoms through photooxidation of Chl (Balachandran and Osmond 1994). Conversely, inhibition of PS2 activity in cucumber mosaic virus (CMV)-infected tobacco plants has been associated with a decrease in the amount of polypeptides of the oxygen-evolving complex

Received 11 December 2003, *accepted* 24 June 2004.
[***]Corresponding author; fax: 0086-571-86049815, e-mail: yu@mail.hz.zj.cn or jqyu@zju.edu.cn
Abbreviations: C_i, intercellular CO_2 concentration; Chl, chlorophyll; F_0, F_m, minimum and maximum Chl fluorescence yield corresponding to open and closed PS2, respectively, after dark pre-treatment; F_0', F_m', minimum and maximum Chl fluorescence yield corresponding to open and closed PS2, respectively, during irradiation; F_v/F_m, the maximal photochemical efficiency of PS2; F_v'/F_m', the efficiency of excitation energy capture by open PS2 reaction centres; g_s, stomatal conductance; J_{max}, maximum electron transport rate contributing to RuBP regeneration; L_s, stomatal limitation; P_{Nsat}, irradiance-saturated net CO_2 assimilation rate; PPFD, photosynthetic photon flux density; PVY^{NTN}, potato virus Y; q_N, non-photochemical quenching coefficient; q_P, photochemical quenching coefficient; RuBP, ribulose-1,5-bisphosphate; RuBPCO, ribulose-1,5-bisphosphate carboxylase/oxygenase; V_{cmax}, the maximum carboxylation velocity of RuBPCO; Φ_{CO_2}, the maximum apparent quantum efficiency for CO_2 assimilation; Φ_{PS2}, quantum yield of electron transport at PS2.
Acknowledgements: We thank the National Natural Science Foundation of China (30325029), 863 Plan Organization of China, Excellent Teacher Foundation of China, and Natural Science Foundation of Zhejiang Province for the financial support.

(Takahashi and Ehara 1992). PVY^{NTN} infection of potato leads to impaired photosynthesis as is the case in other virus diseases (Chia and He 1999, Funayama 2001). It influences the ultrastructure of chloroplasts in primary infected potato leaves (Pompe-Novak *et al.* 2001). The underlying causes remain largely unknown, as do the basis of pathogenicity (Nadderi and Berger 1997a,b, Petrovic *et al.* 1997). It is not certain if impaired photosynthesis results from stomatal limitation or biochemical limitation or photoinhibition or other factors. In this study, we demonstrate how changes in the gas exchange parameters, CO_2 fixation capacity, and Chl fluorescence quenching in plants infected with PVY^{NTN} are related to the impaired photosynthesis.

Materials and methods

Plant and virus materials: Groups of two potato (*Solanum tuberosum* L. cv. Chunzao) plants were grown in a 15 000 cm^3 pot with soils in a greenhouse maintained at 25/20 °C and relative humidity of 80–90 %. A geographical isolate of the potato virus Y^{NTN} (PVY^{NTN}) strain obtained from a highly susceptible potato cv. No. 35 was used. Plants with six fully developed leaves were inoculated with potato virus PVY^{NTN} (Dolenc *et al.* 2000, Milavec *et al*. 2001). After infection, both healthy and viral systemically infected plants were transferred to a growth chamber. The chamber was maintained at 25/20 °C with photosynthetic photon flux density (PPFD) of 500 μmol(photon) m^{-2} s^{-1} and relative humidity of 80–90 %. During the experiment, the pots were watered every 2–3 d with a nutrient solution containing [mM] 6.0 KNO_3, 2.0 $Ca(NO_3)_2$, 1.0 $NH_4H_2PO_4$, and 1.0 $MgSO_4$ (Yu and Matsui 1997). Eighty days later, plants were harvested and weighted. There were twenty Y^{NTN}-infected plants and controls, respectively.

Leaf Chl was extracted in dim light with 80 % acetone in the presence of small amount of $CaCO_3$. The extract was centrifuged at 5 000×*g* for 10 min at 2 °C and the supernatant was further cleared by passing through a 0.45 μm filter. Chls were measured spectrophotometrically using a *Shimazu UV 2100* spectrophotometer (Manetas *et al.* 2002).

Gas exchange measurements: Analyses of the various photosynthetic parameters were carried out in virus-infected plants and in the corresponding controls. The 5th symptomatic leaf from bottom was selected for the measurement of CO_2 assimilation using an infrared gas analyzer (*CIRAS-1*, *PP Systems*, Hitchin, UK). For the measurements of the net photosynthetic rate (P_N), intercellular CO_2 content (C_i), and stomatal conductance (g_s), air temperature, air relative humidity, CO_2 concentration, and PPFD were maintained at 25 °C, 80–90 %, 360 μmol mol^{-1}, and 1 050 μmol(photon) m^{-2} s^{-1}, respectively. Measurements of P_N/PPFD or P_N/C_i were made in descending order from 1 300 to 10 μmol(photon) m^{-2} s^{-1}, and from 1 500 to 10 μmol mol^{-1}, respectively. From the P_N/C_i and P_N/PPFD curves, stomatal limitation (L_s) and true quantum yield of CO_2 assimilation (Φ_{CO_2}) were calculated, respectively (Farquhar and Sharkey 1982). Estimation of the maximum electron transport rate contributing to RuBP (ribulose-1,5-bisphosphate) regeneration (J_{max}) and the maximum carboxylation velocity of RuBPCO (V_{cmax}) were made by fitting a maximum likelihood regression below and above the inflexion of the P_N/C_i response using the method of McMurtrie and Wang (1993).

Chl fluorescence quenching was measured simultaneously using a system that combined the infrared gas analyzer with a *FMS-2* pulse-modulated fluorometer (*Hansatech Instruments*, Norfolk, UK) (Yu *et al.* 2002).

After 15 min dark adaptation, the minimal fluorescence F_0 was measured as the average of the fluorescence signal under a week pulse of amber modulating radiation emitting diode over a 1.8-s period, and maximal fluorescence F_m was measured after a saturating pulse (8 000 μmol m^{-2} s^{-1}) of 0.7 s. The maximum quantum efficiency of PS2 was determined as F_v/F_m, where F_v is the difference between F_0 and F_m. An "actinic light" (600 μmol m^{-2} s^{-1}) was then applied to achieve steady photosystems and to obtain F_s (steady state fluorescence yield). After that, a saturating pulse was applied for 0.7 s to obtained F_m' (light adapted maximal fluorescence). From the measurement, maximum quantum efficiency of PS2 photochemistry (F_v/F_m), the relative quantum efficiency of PS2 electron transport (Φ_{PS2}), the efficiency of excitation energy capture by open PS2 reaction centres (F_v'/F_m'), photochemical quenching (q_P), and non-photochemical quenching (q_N) were determined, respectively (Genty *et al.* 1989).

Results

The first symptoms appeared 8–13 d after inoculation and plant growth was significantly inhibited by the PVY^{NTN} infection. PVY^{NTN}-infected plants initially developed local lesions and later also severe systemic symptoms such as vein necrosis, leaf mosaic, and curling. At the end of the experiment, the average tuber yield for the PVY^{NTN}-infected plants was only 79.7 % of the control plants, respectively (values not shown).

The changes in Chl content and gas exchange parameters with the development of virus infection in potato plants are shown in Fig. 1. P_{Nsat} and g_s of the healthy leaves decreased gradually. The virus-infected leaves

showed reduced P_{Nsat} and g_s in comparison with the healthy leaves from 20 d after the infection. Twenty days after infection, P_{Nsat} decreased by 27.4 % as compared to control. C_i did not change until 60 d after the infection of the experiment, but no significant differences in C_i were observed between the healthy leaves and diseased leaves. The decrease in Chl content developed later than that in P_{Nsat} and significant differences between two treatments were observed only on 60 d after infection.

Analyses of P_N/C_i curves throughout the experiment revealed that viral infection markedly decreased maximum carboxylation velocity of RuBPCO (V_{cmax}) and

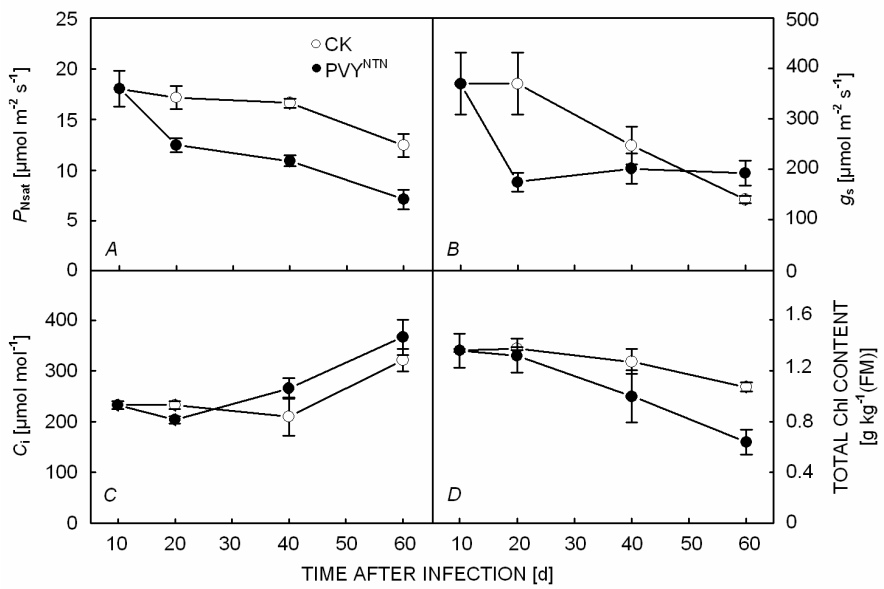

Fig. 1. Effects of potato virus Y^{NTN} on the (*A*) photon-saturated net photosynthetic rate (P_{Nsat}), (*B*) stomatal conductance (g_s), (*C*) intercellular CO_2 concentration (C_i), and (*D*) chlorophyll (Chl) content for control (○) and viral infected (●) potato leaves. Means of three measurements (three seedlings) with standard deviations shown by the vertical bars. Leaf temperature was maintained at 25±0.5 °C with 360 µmol(CO_2) mol^{-1} and 1 050 µmol m^{-2} s^{-1} incident PPFD for the measurement.

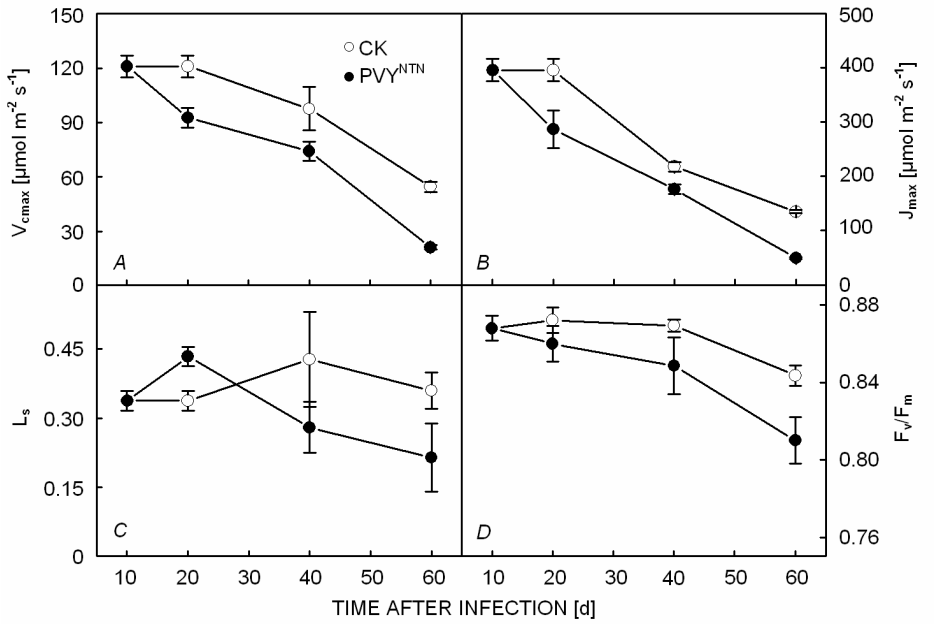

Fig. 2. Effects of potato virus Y^{NTN} infection on (*A*) maximum carboxylation velocity of RuBPCO (V_{cmax}), (*B*) maximum potential rate of electron transport contributed to RuBP regeneration (J_{max}), (*C*) stomatal limitation (L_s), and (*D*) maximum photochemical efficiency (F_v/F_m) for control (○) and viral infected (●) potato leaves. Leaf temperature was maintained at 25±0.5 °C with 1 050 µmol m^{-2} s^{-1} incident PPFD for the measurement.

maximum potential rate of electron transport contributing to RuBP regeneration (J_{max}). Twenty days after infection, V_{cmax} and J_{max} for the viral infected leaves decreased by 23.4 and 27.0 %, respectively, as compared to control (Fig. 2). Stomatal limitation (L_s) increased at the early stage but decreased at the later stage after viral infection.

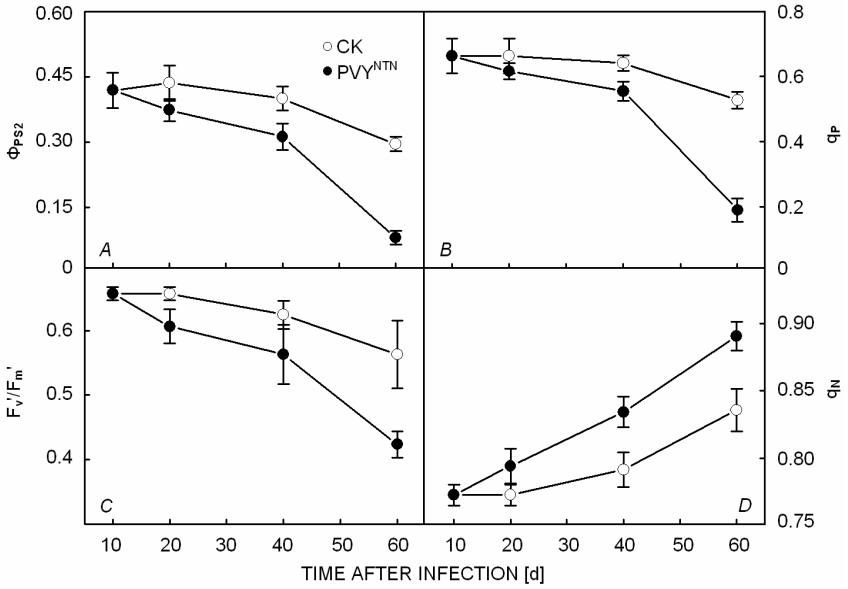

Fig. 3. Effects of potato virus Y^{NTN} infection on (*A*) quantum efficiency of PS2 (Φ_{PS2}), (*B*) photochemical quenching coefficient (q_P), (*C*) the efficiency of excitation capture by open PS2 centres (F_v'/F_m'), and (*D*) non-photochemical quenching coefficient (q_N) for control (○) and potato virus Y infected (●) potato plants. Means of three replicates with standard errors shown by vertical bars.

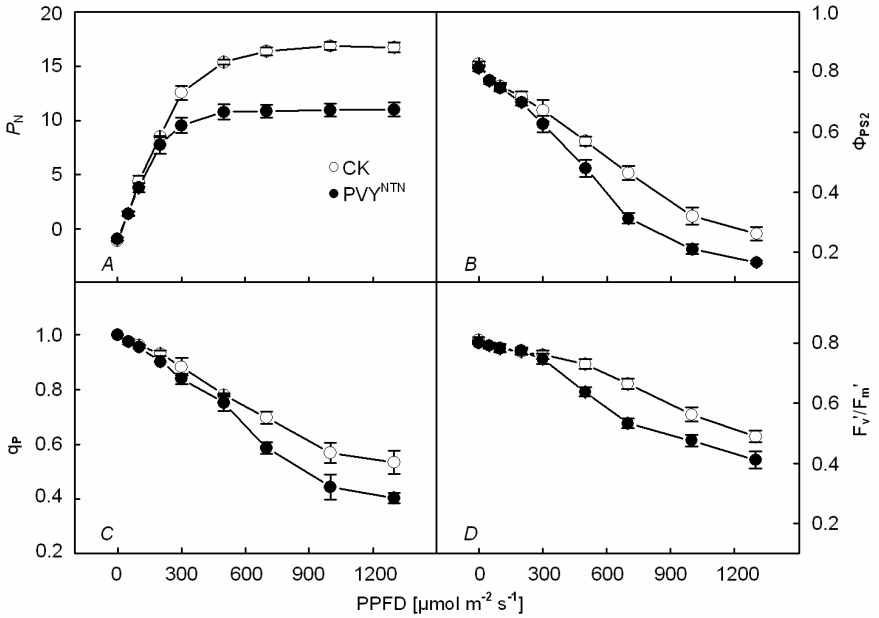

Fig. 4. Response of (*A*) net assimilation rate (P_N), (*B*) quantum efficiency of PS2 (Φ_{PS2}), (*C*) photochemical quenching coefficient (q_P), and (*D*) the efficiency of excitation capture by open PS2 centres (F_v'/F_m') to decreasing PPFD for control (○) and potato virus Y^{NTN} infected (●) potato plants. Measurement was carried out 40 d after viral infection. Leaf temperature was maintained at 25±0.5 °C with 360 μmol(CO_2) mol^{-1}. Means of three replicates with standard errors shown by vertical bars.

A slight but significant decrease in F_v/F_m was observed 60 d after viral infection (Fig. 2*D*). Φ_{PS2}, F_v'/F_m', and q_P decreased with plant growth but the declines were much earlier in infected leaves than in healthy leaves. In contrast, q_N significantly increased with plant growth and the trend was more apparent in diseased

leaves (Fig. 3).

P_N increased almost linearly at the PPFD range of 0–300 μmol(photon) m^{-2} s^{-1}, then became saturated both in healthy and diseased leaves. Chl fluorescence quenching parameters in response to incident PPFD are also shown in Fig. 4. Φ_{PS2}, q_P, and F_v'/F_m' all decreased with increasing PPFD in both types of leaves. However, healthy leaves showed significantly higher Φ_{PS2}, q_P, and F_v'/F_m' values than the infected leaves, except those measured at low PPFD.

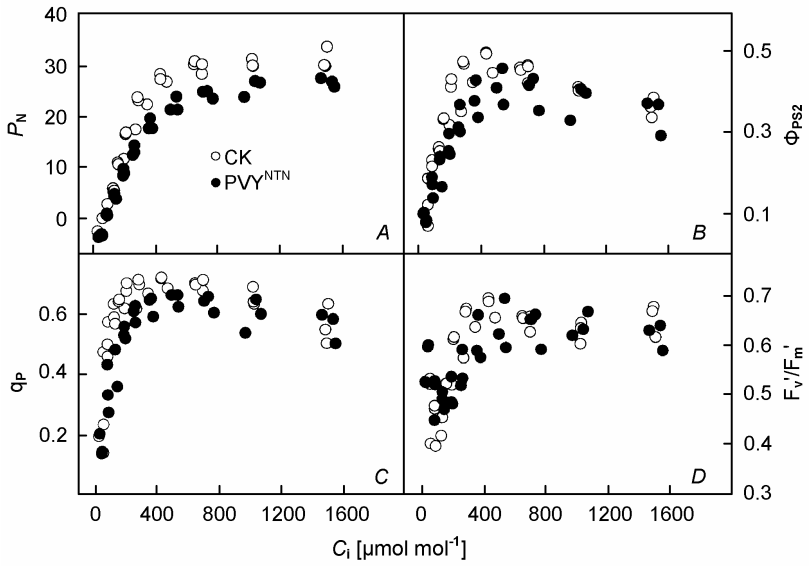

Fig. 5. Response of (*A*) net photosynthetic rate (P_N), (*B*) quantum efficiency of PS2 (Φ_{PS2}), (*C*) photochemical quenching coefficient (q_P), and (*D*) efficiency of excitation capture by open PS2 centres (F_v'/F_m') to decreasing intercellular CO_2 concentration (C_i) for control (○) and potato virus Y^{NTN} infected (●) potato plants. Measurement was carried out 40 d after viral infection. Leaf temperature was maintained at 25±0.5 °C with 1 050 μmol m^{-2} s^{-1} incident PPFD. Means of three replicates with standard errors shown by vertical bars.

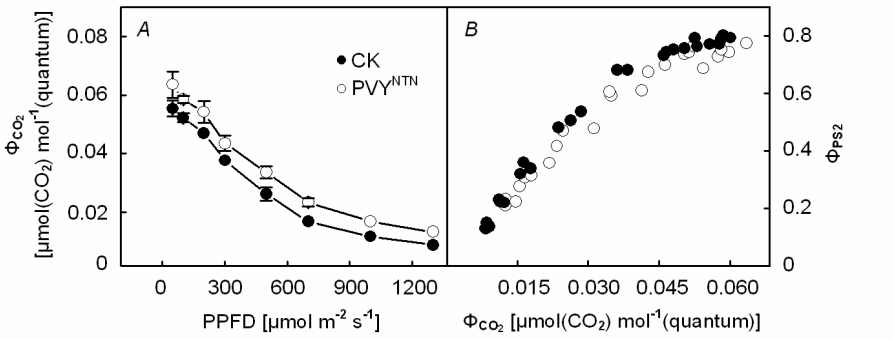

Fig. 6. Relationship between (*A*) PPFD and true quantum yield for CO_2 assimilation (Φ_{CO_2}) and (*B*) Φ_{CO_2} and quantum efficiency of PS2 electron transport (Φ_{PS2}) for healthy (○) and potato virus Y^{NTN} infected potato leaves (●). Measurement was carried out 40 d after viral infection.

P_N, Φ_{PS2}, q_P, and F_v'/F_m' all sharply responded to C_i in the range of 0–500 μmol(CO_2) mol^{-1} and then they reached a plateau or declined slightly. The values of P_N, Φ_{PS2}, q_P, and F_v'/F_m' were generally higher for healthy leaves than for the diseased leaves although there were some exceptions (Fig. 5).

Φ_{CO_2} decreased with increased PPFD (Fig. 6*A*). At each given PPFD, Φ_{CO_2} for diseased leaves was significantly lower than that for healthy leaves. When Φ_{PS2} was plotted against Φ_{CO_2}, a close relation was found (Fig. 6*B*). Viral infection slightly increased the ratio of Φ_{PS2}/Φ_{CO_2}, indicating that the infected plants needed a higher rate of photosynthetic electron supply for CO_2 assimilation in comparison to healthy leaves.

Discussion

Reduced photosynthesis as a result of viral infection is a well-recognized phenomenon (Goodman *et al*. 1986). In agreement with previous studies, our study showed that P_{Nsat} decreased with disease progression (Fig. 1). The reduced P_{Nsat} was not accompanied by a significant decrease in C_i, suggesting that stomata were the limiting factor for the reduced photosynthetic rate (Caemmerer and Farquhar 1981). Moreover, the substantial decrease in P_{Nsat} was not accompanied by significant changes in Chl content and F_v/F_m at the early stage, suggesting that the reduced photosynthesis in diseased leaves could not also be attributed to changes in Chl contents and photoinhibition (Baker *et al.* 1997).

Changes accompanying P_{Nsat} (Fig. 1) were significant decreases in V_{cmax} and J_{max} (Fig. 2), indicating that viral infection greatly reduced the carboxylation efficiency and the ability to regenerate RuBP. RuBP regeneration could be limited either by the inability of electron transport to supply reductants and ATP or by an inactivation or loss of Calvin cycle enzymes other than RuBPCO (Baker *et al.* 1997). The pronounced decrease in J_{max}, that occurred 20 d after infection, was not accompanied by changes of similar magnitude in Φ_{PS2} and F_v/F_m. Hence the virus might interfere with the enzymatic process in the Calvin cycle and lead to reduction in the ability to regenerate RuBP. Significant decreases in the activities of some enzymes in Calvin cycle have been observed in TMS-infected tobacco plants (Montalbini and Lupattelli 1989). Our result is in agreement also with the argument of Pompe-Novak *et al.* (2001) that the decreased P_N caused by PVY^{NTN} is a consequence of changes at the biochemical level.

At the late stage of the experiment, significant reductions in P_{Nsat}, V_{cmax}, and J_{max} were accompanied by similar decreases in Φ_{PS2}, q_P, and F_v'/F_m'. No apparent changes in F_v/F_m were observed throughout the experiment, indicating that no photo-damage to PS2 reaction centres occurred. Φ_{PS2} is the product of $F_v'/F_m' \times q_P$. Since both q_P and F_v'/F_m' decreased in proportion to Φ_{PS2}, the reduced Φ_{PS2} was attributed both to a reduction in the fraction of open reaction centres and a reduction in the efficiency of excitation energy capture in PS2, as a result of photo-protective thermal dissipation of excess excitation energy, as observed in PMMoV-infected *Nicotiana benthamiana* plants (Rahoutei *et al.* 2000). We attributed the decreases in q_P to decreases in the consumption of reductant and ATP since negligible photodamage to PS2 occurred (F_v/F_m remained close to 0.8–0.9). Accordingly, virus-induced decrease in Φ_{PS2} is attributed to 'down-regulation' of the electron transport and photodamage to PS2 reaction centres is not a primary factor in the depression of CO_2 assimilation. The decrease in the demand for ATP and reductants would lead to the closure of PS2 reaction centres. Many studies have demonstrated lower photosynthetic electron transport rates in infected plants, especially at the PS2 level (Reinero and Beachy 1989, Rahoutei *et al.* 2000). TMV- and CMV-coat proteins (CP) accumulate in the chloroplast and are bound to the PS2 complex in viral infected leaves, resulting in a decreased PS2 electron transport and a decrease in the amount of polypeptides of oxygen-evolution complex (Reinero and Beachy 1989, Takahashi and Ehara 1992).

Biotic and abiotic stresses also change the ratio of Φ_{PS2}/Φ_{CO2}, an indicator of electron flow (Ort and Baker 2002). Slight increases in Φ_{PS2}/Φ_{CO2} observed in virus-infected leaves (Fig. 6*B*) suggested that viral infection increased the rate of photosynthetic electron transport to alternative electron sinks such as nitrate reaction, Mehler reactions, and photorespiration. In fact, increased activity of Mehler reactions was observed in PVY^{NTN}-infected leaves (Milavec *et al.* 2001). This is generally in agreement with the abiotic stress such as chill and drought stresses that greatly increase the amount of electrons needed to assimilate one CO_2 and the activities of some Mehler pathway enzymes (Ort and Baker 2003).

References

Baker, N.R., Nogues, S., Allen, D.J.: Photosynthesis and photoinhibition. – In: Lumsden, P.J. (ed.): Plants and UV-B: Response to Environmental Change. Pp. 95-111. Cambridge University Press, Cambridge 1997.

Balachandran, S., Hurry, V.M., Kelley, S.E., Osmond, C.B., Robinson, S.A., Rohozinski, J., Seaton, G.G.R., Sims, D.A.: Concepts of plant biotic stress. Some insights into the stress physiology of virus-infected plants, from the perspective of photosynthesis. – Physiol. Plant. **100**: 203-213, 1997.

Balachandran, S., Osmond, C.B.: Susceptibility of tobacco leaves to photoinhibition following infection with two strains of tobacco mosaic virus under different light and nitrogen nutrition regimes. – Plant Physiol. **104**: 1051-1057, 1994.

Balachandran, S., Osmond, C.B., Makino, A.: Effects of two strains of tobacco mosaic virus on photosynthetic characteristics and nitrogen partitioning in leaves of *Nicotiana tabacum* cv. Xanthi during photoacclimation under two nitrogen nutrition regimes. – Plant Physiol. **104**: 1043-1050, 1994.

Caemmerer, S. von, Farquhar, G.D.: Some relations between the biochemistry of photosynthesis and the gas exchange of leaves. – Planta **153**: 376-387, 1981.

Chia, T.F., He, J.: Photosynthetic capacity in *Oncidium* (*Orchidaceae*) plants after virus eradication. – Environ. exp. Bot. **42**: 11-16, 1999.

Dolenc, J., Vilhar, B., Dermastia, M.: Systematic infection with potato Y^{NTN} alters the structure and activity of the shoot apical meristem in a susceptible potato cultivar. – Physiol. mol. Plant Pathol. **56**: 33-38, 2000.

Farquhar, G.D., Sharkey, T.D.: Stomatal conductance and photosynthesis. – Annu. Rev. Plant Physiol. **33**: 317-345, 1982.

Funayama, N.S.: Ecophysiology of virus-infected plants: A case study of *Eupatorium makinoi* infected by geminivirus. – Plant Biol. **3**: 251-262, 2001.

Funayama, S., Sonoike, K., Terashima, I.: Photosynthetic properties of leaves of *Eupatorium makinoi* infected by a geminivirus. – Photosynth. Res. **53**: 253-261, 1997.

Funayama, S., Terashima, I.: Effects of geminivirus infection and growth irradiance on the vegetative growth and photosynthetic production of *Eupatorium makinoi.* – New Phytol. **142**: 483-494, 1999.

Genty, B., Briantais, J.-M., Baker, N.R.: The relationship between the quantum yield of photosynthetic electron transport and quenching of chlorophyll fluorescence. – Biochim. biophys. Acta **990**: 87-92, 1989.

Goodman, R.N., Kiraly, Z., Wood, K.R.: Photosynthesis. – University of Missouri Press, Columbia 1986.

Manetas, Y., Drinia, A., Petropoulou, Y.: High contents of anthocyanins in young leaves are correlated with low pools of xanthophyll cycle components and low risk of photoinhibition. – Photosynthetica **40**: 349-354, 2002.

McMurtrie, R.E., Wang, Y.-P.: Mathematical models of the photosynthetic response of tree stands to rising CO_2 concentrations and temperatures. – Plant Cell Environ. **16**: 1-13, 1993.

Milavec, M., Ravnikar, M., Kovac, M.: Peroxidases and photosynthetic pigments in susceptible potato infected with potato virus Y^{NTN}. – Plant Physiol. Biochem. **39**: 891-898, 2001.

Montalbini, P., Lupattelli, M.: Effects of localized and systemic tobacco mosaic virus infection on some photochemical and enzymatic activities of isolated tobacco chloroplasts. – Physiol. mol. Plant Pathol. **34**: 147-162, 1989.

Nadderi, M., Berger, P.H.: Effects of chloroplast targeted potato virus Y coat protein on transgenic plants. – Physiol. mol. Plant Pathol. **50**: 67-83, 1997a.

Nadderi, M., Berger, P.H.: Pathogenesis-related protein 1a is induced in potato virus Y-infected plants as well as by coat protein targeted to chloroplasts. – Physiol. mol. Plant Pathol. **51**: 41-44, 1997b.

Ort, D.R., Baker, N.R.: A photoprotective role for O_2 as an alternative electron sink in photosynthesis? – Curr. Opin. Plant Biol. **5**: 193-198, 2002.

Osmond, C.B., Daley, P.F., Badger, M.R., Luttge, U.: Chlorophyll fluorescence quenching during photosynthetic induction in leaves of *Abutilon striatum* Dicks. infected with abutilon mosaic virus, observed with a field-portable imaging system. – Bot. Acta **111**: 390-397, 1998.

Petrovic, N., Miersch, O., Ravnikar, M., Kovac, M.: Potato virus Y^{NTN} alters the distribution and concentration of endogenous jasmonic acid in potato plants grown in vitro. – Physiol. mol. Plant Pathol. **50**: 237-244, 1997.

Pompe-Novak, M., Wrischer, M., Ravnikar, M.: Ultrastructure of chloroplasts in leaves of potato plants infected by potato virus Y^{-NTN}. – Phyton-Ann. Rei Bot. **41**: 215-226, 2001.

Rahoutei, J., Garcia-Luque, I., Baron, M.: Inhibition of photosynthesis by viral infection: Effect on PS2 structure and function. – Physiol. Plant. **110**: 286-292, 2000.

Reinero, A., Beachy, R.N.: Reduced photosystem II activity and accumulation of viral coat protein in chloroplasts of leaves infected with tobacco mosaic virus. – Plant Physiol. **89**: 111-116, 1989.

Swiech, R., Browning, S., Molsen, D., Stenger, D.C., Holbrook, G.P.: Photosynthetic responses of sugar beet and *Nicotiana benthamiana* Domin. infected with beet curly top virus. – Physiol. mol. Plant Pathol. **58**: 43-52, 2001.

Takahashi, H., Ehara, Y.: Changes in the activity and the polypeptide composition of the oxygen-evolving complex in photosystem II of tobacco leaves infected with cucumber mosaic virus strain Y. – Mol. Plant Microbe Interactions **5**: 269-272, 1992.

Wolf, S., Millatiner, A.: Effect of tobacco mosaic virus movement protein on photosynthesis in transgenic tobacco plants. – J. Plant Physiol. **156**: 253-258, 2000.

Yu, J.Q., Matsui, Y.: Effects of root exudates and allelochemicals on ion uptake by cucumber seedlings. – J. chem. Ecol. **23**: 817-827, 1997.

Yu, J.Q., Zhou, Y.H., Huang, L.F., Allen, D.: Chill-induced inhibition of photosynthesis: genotypic variation within *Cucumis sativus*. – Plant Cell Physiol. **43**: 1182-1188, 2002.